The Canadian Mineralogist
Vol. 43, pp. 367-385 (2005)

THE SIGNIFICANCE OF PLAGIOCLASE-DOMINANT CORONAS ON GARNET, WENATCHEE BLOCK, NORTHERN CASCADES, WASHINGTON, U.S.A.

Harold H. STOWELL[§] and Ellen STEIN

Department of Geological Sciences, The University of Alabama, Tuscaloosa, Alabama 35487-0338, U.S.A.

Abstract

Coronas on garnet, reported from numerous localities throughout the North Cascades Crystalline Core, have been interpreted to record rapid exhumation, associated with regional late Cretaceous and early Paleogene unroofing. Granodiorite dikes adjacent to tonalite and gabbro bodies, in the southern and central Cascades Core, contain fine-grained plagioclase-dominant coronas cored by garnet. Locally, these coronas were strongly deformed into ellipsoids with aspect ratios of 1:1.8:3.1. The matrix assemblage around coronas is biotite + plagioclase + quartz + ilmenite + apatite + zircon ± allanite ± muscovite ± sillimanite. Garnet is strongly zoned with simple or complex patterns. Simply zoned garnet shows a core-to-rim variation: 70–81% almandine, 7–10% pyrope, 10–2% spessartine, 14–8% grossular, with no reversals in zoning near the rim (*e.g.*, no Mn increase), and is interpreted as metamorphic growth-zoning. Examples of complexly zoned garnet show core-to-rim zoning indicative of diffusive re-equilibration of central grains, and overgrowth of younger grains. Plagioclase in all samples is mostly anhedral and unzoned, but many grains include small $An_{60–70}$ cores with oscillatory zoning that are interpreted as relict phenocrysts. Plagioclase composition and texture, and phase-equilibria constraints on mineral reactions, are most compatible with garnet growth by replacement of igneous high-An plagioclase plus chlorite by "new" lower-Ca (An_{40}) plagioclase and garnet. Incomplete progress of the reaction, as indicated by persistence of coronas and "relics" of primary plagioclase, may be due to an abrupt decrease in temperature, with possible loss of fluid. The textural and mineral-chemical data support the interpretation that these plagioclase-dominant coronas around garnet from the central Cascades Core developed during prograde M_3 metamorphism, after intrusion of the Mount Stuart batholith, not late decompression.

Keywords: plagioclase-dominant corona on garnet, decompression, depletion halo, North Cascades, Washington.

Sommaire

La présence de couronnes développées sur le grenat, telle que décrites à plusieurs localités du socle cristallin de la partie nord des Cascades, aux Etats-Unis, a été interprétée en termes d'une exhumation rapide, associée au soulèvement régional à la fin du Crétacé et au Paléogène précoce. Les filons de granodiorite voisins des massifs de tonalite et de gabbro, dans les parties sud et centrale de cette même ceinture, contiennent des couronnes de plagioclase à grains fins sur cristaux de grenat. Ici et là, ces couronnes sont fortement déformées, et donc devenues des ellipses, avec un rapport des aspects de 1:1.8:3.1. La matrice autour des couronnes contient l'assemblage biotite + plagioclase + quartz + ilménite + apatite + zircon ± allanite ± muscovite ± sillimanite. Le grenat est fortement zoné, avec un tracé de composition simple ou complexe. Le grenat simplement zoné contient une variation du coeur à la bordure: 70–81% almandin, 7–10% pyrope, 10–2% spessartine, 14–8% grossular, sans inversions en zonation près de la bordure (c'est-à-dire, sans augmentation de Mn), et serait dû à une zonation au cours de la croissance métamorphique. Les exemples de zonation complexe résulteraient de ré-équilibrage des grains du centre par diffusion, et d'une surcroissance sur les grains précoces. Le plagioclase dans tous les échantillons est surtout xénomorphe et homogène, mais plusieurs grains ont des inclusions de petits noyaux de composition $An_{60–70}$ ayant une zonation oscillatoire, que nous interprétons comme des reliques de phénocristaux. La composition et la texture du plagioclase, et les contraintes exercées par les réactions parmi les minéraux venant des équilibres de phases, sont en général davantage compatibles avec une croissance du grenat par remplacement du plagioclase calcique igné avec chlorite par un "nouveau" plagioclase à plus faible teneur en Ca (An_{40}) avec grenat. Une progression incomplète de la réaction, comme l'indique la persistance de couronnes et de "reliques" de plagioclase primaire, pourrait témoigner d'une diminution abrupte de la température, peut-être même avec perte de fluide. Les observations texturales et les données sur la composition des minéraux étayent l'interprétation voulant que ces couronnes à dominance de plagioclase autour du grenat dans la ceinture centrale du socle des Cascades se sont développées au cours de l'épisode M_3 de métamorphisme prograde, après la mise en place du batholite de Mount Stuart, et non tardivement, lors de la décompression.

(Traduit par la Rédaction)

Mots-clés: couronne de plagioclase sur grenat, décompression, auréole d'épuisement, socle des Cascades, Washington.

§ *E-mail address*: hstowell@wgs.geo.ua.edu

Introduction

Corona textures have a tremendous appeal to geologists owing to their beauty and potential to provide insights into geological processes (*e.g.*, Barker 1990). Plagioclase-dominant coronas on garnet in high-grade rocks are generally attributed to high-temperature near-isothermal decompression that destabilized garnet relative to plagioclase (*e.g.*, Barker 1990). However, quartzofeldspathic coronas around ferromagnesian porphyroblasts also have been interpreted as depletion haloes (*e.g.*, Spry 1969). Coronas cored by garnet are widespread throughout the crystalline rocks of the North Cascades (Figs. 1, 2; *e.g.*, Misch & Onyeagocha 1976, Longtine 1991, Whitney 1992, Paterson *et al.* 1994, Wernicke & Getty 1997, Whitney *et al.* 1999). Corona textures in migmatitic gneiss of the North Cascades (Skagit Gneiss) comprise plagioclase plus hornblende around garnet, or cordierite around garnet, and have been ascribed to high-temperature decompression (Whitney 1992, Wernicke & Getty 1997). Some corona textures southwest of the Skagit Gneiss, in the Wenatchee and Chelan blocks of the North Cascades, also have been ascribed to decompression (*e.g.*, Miller *et al.* 2000, Stein & Stowell 2002). Other corona textures in amphibolite and schist from the Wenatchee block have been interpreted as depletion haloes (Longtine 1991, Winter 2001). In this paper, we present mineral chemical data and a growth model for plagioclase-dominant coronas from the Wenatchee block. Euhedral to subhedral crystals of garnet, garnet zoning, plagioclase textures, and mass-balance constraints are most compatible with garnet growth by consumption of chlorite during prograde metamorphism. The assemblage chlorite + early high-Ca plagioclase is interpreted to have reacted to produce lower-anorthite plagioclase plus garnet. This likely produced a depletion-halo type of corona by consumption of ferromagnesian minerals around the garnet porphyroblasts.

Regional Setting

The Cordilleran Coast Plutonic Complex comprises the roots of a mid-Cretaceous to Paleogene magmatic arc and orogenic belt that extends from Washington to the Yukon Territory. This arc separates the Intermontane superterrane on the east from the Insular superterrane on the west (Monger *et al.* 1982). The North Cascades Crystalline Core (Cascades Core) in Washington is the southernmost exposure of the Coast Plutonic Complex (Fig. 1). Middle to Late Cretaceous metamorphism in the Coast Plutonic Complex occurred during or after crustal thickening, attributed to Cretaceous collision of the Intermontane and Insular superterranes (Miller 1985, Paterson *et al.* 1994). In the Cascades Core, the Ingalls Ophiolite Complex was thrust over the Chiwaukum Schist (Miller 1985, Paterson *et al.* 1994) (Fig. 2). Crustal thickening and subsequent dextral slip were accompanied by intrusion of tonalite, granodiorite, and diorite plutons and metamorphism. Early regional metamorphism may predate emplacement of the Ingalls ophiolite complex and pluton emplacement during the mid-Cretaceous. Metamorphism and pluton emplacement culminated in the western and central parts of the complex at around 90 Ma.

The Cascades Core consists of 96–45 Ma plutonic and medium- to high-grade metamorphic rocks offset from the Canadian Coast Plutonic Complex by mid-Tertiary dextral strike-slip motion along the Straight Creek fault (Umhoefer & Miller 1996). The northwest–southeast-trending Entiat fault (Eocene) separates the Cascades Core into the Chelan block to the northeast and the Wenatchee block to the southwest. The Wenatchee block contains medium- to high-grade schist and gneiss of the Nason and Chelan Mountains terranes, intruded by a suite of predominantly 90–96 Ma plutons (Fig. 2), whereas rock of the Chelan Mountains terrane in the Chelan block are intruded by the 90–96 Ma suite and younger Cretaceous to early Tertiary (*ca.* 45 Ma) plutons (Miller *et al.* 1989, Haugerud *et al.* 1991). Argon cooling ages indicate that high-grade metamorphism in the Wenatchee block ceased in the late Cretaceous (Engels *et al.* 1976, Tabor *et al.* 1987, Magloughlin 1993, Evans & Davidson 1999). The Cascades Core experienced contractional orogenesis in the mid-Cretaceous, resulting in a prominent northwest–southeast-trending fabric. Northeast–southwest-directed compression resulted in southwest-directed thrusting, shearing, and southwest-vergent folding (Paterson & Miller 1998, Miller *et al.* 2000). This compression and subsequent extension resulted in development of prominent shear-zones, including the White River shear-zone, a terrane-bounding reverse shear-zone that separates the Napeequa Complex and Swakane Gneiss of the Chelan Mountains terrane from the Nason terrane to the southwest (Figs. 1, 2).

The Wenatchee block is underlain by five metamorphic units; from northeast to southwest, these are the Swakane Gneiss, Napeequa Complex, Chiwaukum Schist, Nason Ridge Migmatitic Gneiss (within the Chiwaukum Schist), and Ingalls Ophiolite Complex (Fig. 3). These largely metasedimentary units are intruded by pre- to syntectonic diorite, tonalite, and granodiorite that range in age from 96 to 90 Ma (Miller *et al.* 2003). The southern end of the Wenatchee block is dominated by the Mount Stuart batholith, a polyphase gabbro, tonalite, and granodiorite complex comprising two large and several smaller bodies (Figs. 2, 3). The U–Pb ages determined on zircon indicate that the batholith was constructed over 5.5 m.y. from *ca.* 96.5 to *ca.* 91.0 Ma (Miller *et al.* 2003). Three metamorphic events, M_1 to M_3 (Table 1), have been identified in the southern and central Wenatchee block (Plummer 1980, Evans & Berti 1986, Paterson *et al.* 1994, Evans & Davidson 1999, Stowell & Tinkham 2003). The earliest metamorphic minerals that have been identified, hornblende and garnet (M_1), predate intrusion of the 96–90 Ma plutons. Andalusite, common near several late Cretaceous plutons (*e.g.*, the Mount Stuart batholith), grew during contact metamorphism that is defined as M_2 (Evans & Berti 1986, Evans & Davidson 1999). Locally, M_2 andalusite is replaced by M_3 kyanite or sillimanite, staurolite, and garnet. Regional metamorphic rocks away from plutons, *e.g.*, north of the Mount Stuart in the Nason Ridge Migmatitic Gneiss (formerly Banded Gneiss) (Tabor *et al.* 2002), contain sillimanite or kyanite. Timing of mineral growth in these rocks has been controversial (Evans & Berti 1986); however, recent work (Tinkham 2002, Stowell & Tinkham 2003) supports the interpretation of Evans & Davidson (1999) that these mineral assemblages (M_3) postdate intrusion of the

TABLE 1. SUMMARY OF METAMORPHIC EVENTS IN THE NORTH CASCADES OF WASHINGTON

	Metamorphic and tectonic events	Pressure (kbar)	Metamorphic facies	Time (Ma)
M_1	Regional metamorphism[1]	3–6?	≤ amphibolite?	103–143[2]
M_2	Contact metamorphism at low pressure (andalusite) in aureoles around Late Cretaceous plutons (*e.g.*, the Mount Stuart batholith)	< 2–4	≤ amphibolite	93–96
M_3	Regional metamorphism at medium to high pressure	6 – ~9	≤ upper amphibolite	87–85

[1] Regional extent, and temperatures and pressures are poorly known. However, M_1 amphibole was described in Paterson *et al.* (1994).
[2] Age range is based on garnet Sm–Nd chronology with large uncertainties (Magloughlin 1993, Chace *et al.* 1998).

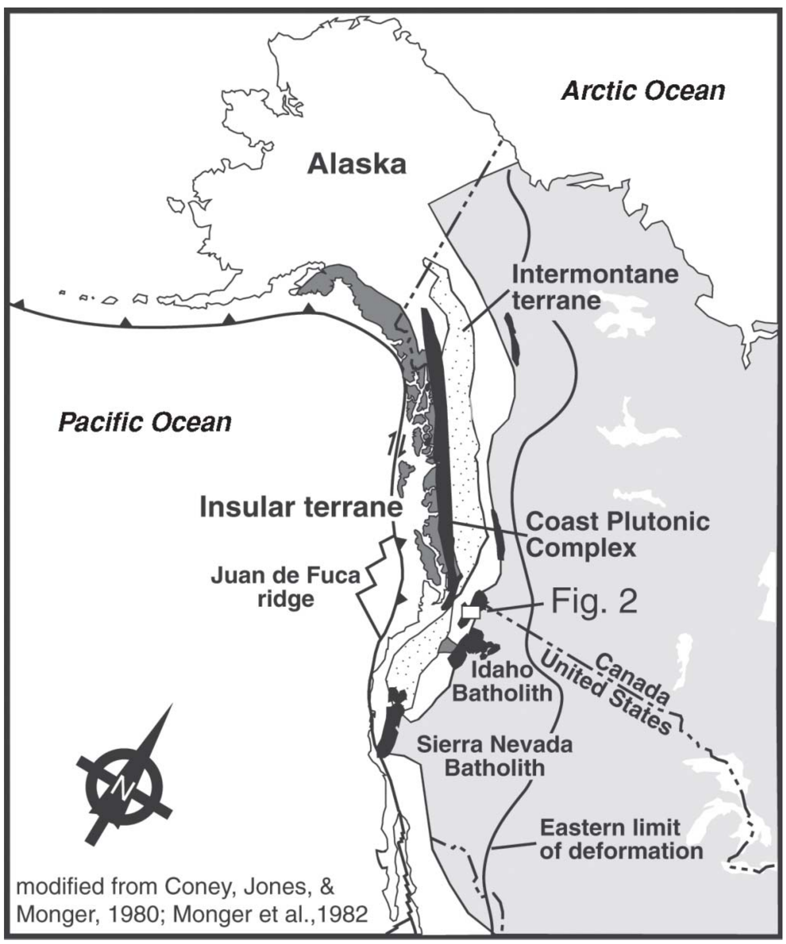

FIG. 1. Generalized tectonic map of the northwestern North American Cordillera with major terranes, batholiths, and fault zones. The North Cascades Core can be seen at the southern end of the Coast Plutonic Complex in north-central Washington. The grey area east of the Cordillera indicates the North American craton.

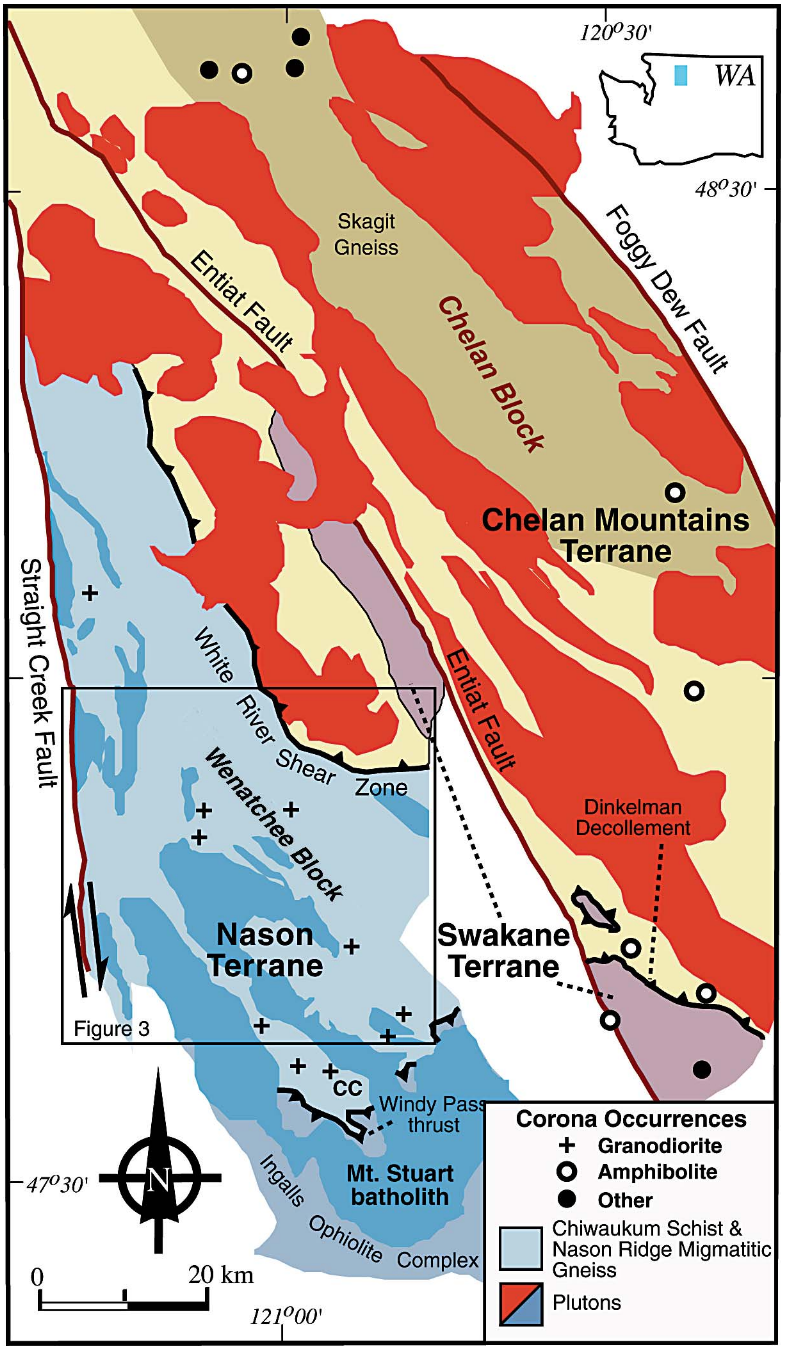

FIG. 2. Generalized map of terranes in the Washington North Cascades Core, with compilation of corona localities in the literature (Longtine 1991, Whitney 1992, Wernicke & Getty 1997, Miller *et al.* 2000, Stein & Stowell 2002) and new localities. Details of the geology are modified from Tabor *et al.* (1982, 1987, 1993, 2002).

Mount Stuart batholith. Thermobarometry (*e.g.,* Brown & Walker 1993, Paterson *et al.* 1994, Evans & Davidson 1999) indicates that pressures recorded during metamorphism generally increase from approximately 3 kbar in the southwest, to >8 kbar in the northeast (Fig. 3). Corona-bearing dike samples discussed below are hosted by andalusite-bearing, kyanite after andalusite-bearing, or sillimanite-bearing pelitic Chiwaukum Schist close to the northern margin of the Mount Stuart batholith.

Late Cretaceous to Tertiary metamorphism along the western flank of the Coast Plutonic Complex in British Columbia and southeastern Alaska is generally attributed to thickening of the crust (*e.g.*, Stowell & Crawford 2000). However, there has been considerable controversy over the cause of M_3 regional metamorphism in the Cascades Core (*e.g.*, Haugerud *et al.* 1994). This 87–85 Ma metamorphism (Stowell & Tinkham 2003) postdates intrusion of *ca.* 94 Ma plutons and has been attributed to thrust thickening of the crust (Monger *et al.* 1982, Whitney & McGroder 1989, McGroder 1991, Whitney *et al.* 1999) or magma loading by now-eroded plutons (Brown & Walker 1993). Further elucidation of the metamorphic P–T paths, including portions recorded in coronas, is important for refining tectonic interpretations.

Dike Textures and Plagioclase-Dominant Coronas on Garnet

Plagioclase-rich coronas on garnet are found in amphibolite, granitic dikes, and other rocks across the North Cascades (Fig. 2). In this paper, we present

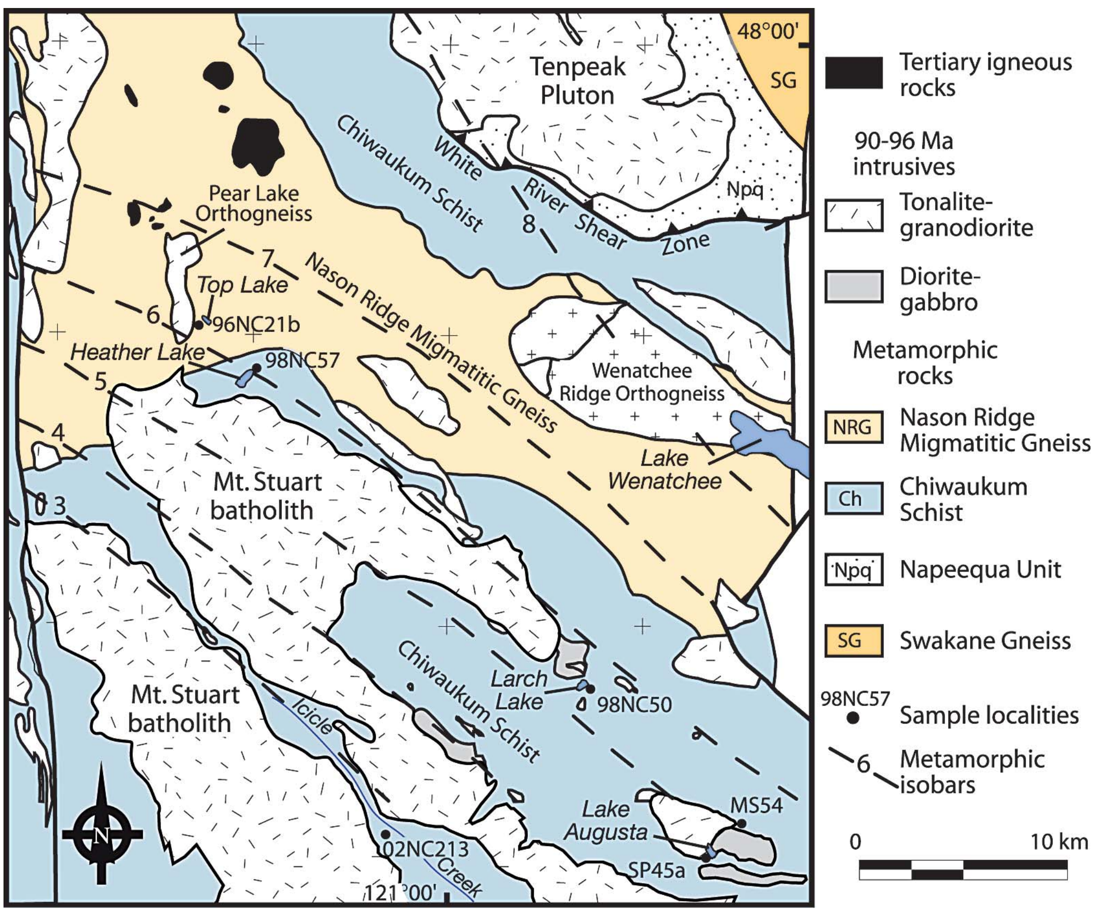

FIG. 3. Geological map of the Wenatchee block of the North Cascades, with "plagioclase on garnet" corona localities discussed herein. Geological units are modified from Tabor *et al.* (1982, 1987, 1993, 2002). Metamorphic pressure (isobars) estimates are from Brown & Walker (1993). Limited geochronology for minerals formed during peak metamorphism indicate that some or all of these pressures correspond to M_3 conditions (Tinkham 2002, Stowell & Tinkham 2003).

textural, mineral chemical, and model reactions for plagioclase-dominant coronas on garnet found in dikes from the Wenatchee block (Figs. 2, 3). Five samples were collected from dikes adjacent to or near the Mount Stuart batholith (Fig. 3, Table 2). These dikes are granodioritic to tonalitic in composition, on the basis of CIPW norms and alkali *versus* silica ratios (Table 3), and henceforth will be called granodiorite. Most dikes are less than 0.5 m thick and cut across folds and the dominant foliation in the Chiwaukum Schist (Fig. 4). Mineralogy includes garnet, biotite, plagioclase, quartz, and minor retrograde chlorite. Biotite is typically foliated and medium to fine grained. Dikes are spatially related to the Mount Stuart batholith and are similar in composition; therefore, they may be derived from the same magmas. However, the complete lack of amphibole and presence of garnet differentiate the dikes from plutons in the adjacent Mount Stuart batholith. Some low-iron, low-magnesium and high-silica dikes from Icicle Creek, including 02NC213a, contain muscovite and the "fibrolite" variety of sillimanite. In spite of well-developed foliation and extensive recrystallization in most samples, coarse phenocrysts of igneous feldspar with a high Ca content are locally preserved in Lake Augusta samples (SP45a, MS54). Plagioclase-dominant coronas on garnet vary from *ca.* 0.5 cm irregular bodies to strongly deformed lenses >3 cm long, cored by individual crystals of garnet or aggregates of ≤1 mm crystals of garnet.

Mineralogical domains

Corona samples from the granodiorite dikes in the Wenatchee block all contain two mineralogical domains, each of which can be subdivided into two subdomains: (1) corona domain, consisting of (a) the garnet subdomain: individual or polycrystalline garnet + inclusions, and (b) a shell subdomain of plagioclase + quartz ± muscovite, and (2) the matrix domain, consisting of (a) a transitional subdomain: plagioclase + quartz + scant biotite, and (b) a distal subdomain: plagioclase + quartz + relatively more biotite.

Figure 5 shows these mineral domains in sample SP45a from Lake Augusta (Fig. 3). Domain and subdomain boundaries are sharp except between the two matrix subdomains, which are not immediately distinguishable. Measurements on back-scattered electron images, however, reveal that biotite grains in the transitional matrix adjacent to coronas are slightly smaller and less closely spaced than in the remainder of the matrix. In general, the transitional zone is narrow, *ca.* 200 μm or less. Biotite is foliated in all samples except 02NC213a from Icicle Creek.

Garnet occurs only in the corona domain, and biotite occurs only in the matrix domain. All other phases, including accessory minerals, are present in both domains, though their mode and composition typically vary between domains. Virtually all samples contain chlorite in and around some garnet grains. This chlorite is interpreted as being late, on the basis of its occurrence as a thin rim or within fractures. Garnet grains typically contains numerous inclusions of quartz (Fig. 5) and rare accessory phases including ilmenite, apatite, zircon, and allanite.

Coronas (garnet + shell) are approximately triaxial ellipsoids, except in Icicle Creek (Fig. 3) samples (*e.g.*, 02NC213a), where they are nearly spherical. Coronas from SP45a (Lake Augusta) were sectioned parallel to the major, intermediate, and minor axes in order to obtain measurements of the mode of coronas and the length of their long, intermediate, and short axes (Table 4). Such measurements in the case of the longest coronas, which were incomplete in thin section or hand sample, were excluded. Modes may overestimate the area of the corona domain, because trimming the samples intentionally maximized the visibility of garnet at the expense of the matrix. Also, because thin sections are too small to fully encompass many coronas, small coronas were selected, which likely led to overestimates of the diameter of the garnet subdomain at the expense of its surrounding shell. More sophisticated techniques of measurement, *e.g.*, three-dimensional computer-assisted X-ray tomography, would likely produce lower estimates of the mode of the corona domain and possibly higher estimates of the size and mode of the shell subdomain. The proportion of coronas may even be lower in samples from some of the other localities, notably Icicle Creek. Forty-three axial measurements were used to construct the idealized corona in Figure 5d. The measurement problems described above indicate that the long axis may be underestimated relative to the other axes. Coronas are up to 8 cm long; however, typically, they are 1–2 cm in maximum dimension.

Coronas typically contain multiple grains of garnet, clustered in the central portion of the domain. In the absence of three-dimensional imaging, the number of garnet grains in typical clusters is poorly known. Locally, coronas contain more than a dozen separate grains. In some samples, garnet grains are closely or loosely intergrown. Garnet grains range in size from *ca.* 1 to 4 mm. In two of the samples (Icicle Creek and Heather Lake; Fig. 3), a mesh of small (<1 mm), subhedral grains of garnet are intergrown around a central roundish garnet *ca.* 3–4 mm in diameter. In the other samples, clustered grains are subequal in size and mostly separate or nearly separate from one another (Fig. 5a).

Quartz and plagioclase grains are generally anhedral and smaller than the garnet. Many plagioclase grains have a complex core–mantle structure that is discussed below in the section on mineral compositions. A few of these complex grains are quite large (>2 cm), with a nearly euhedral core. Biotite grains are generally subhedral and small (<1 mm long in all samples), and are well aligned into a fabric (Fig. 5) subparallel with the fabric in the host rocks. Randomly oriented grains of biotite in sample 02NC213a from Icicle Creek are extremely small (≤0.5 mm in length).

Deformation

The deformation of coronas is obvious in all but one of the samples (02NC213, Icicle Creek), with biotite defining a strong foliation in the matrix. Viewed along planes that include their longest axes, coronas may superficially resemble pressure shadows on porphyroblasts, with biotite grains in the transitional matrix wrapping around the corona (Fig. 5). Unlike pressure shadows, however, the coronas completely surround garnet grains, and there is no contact between biotite and the garnet. The distance across deformed plagioclase coronas, *i.e.*, separation between garnet and matrix, is greatest along the longest coronal axis and smallest along the shortest axis. This distance in the essentially undeformed sample (Icicle Creek) is approximately the same in all three directions.

Mineral Compositions and Zoning

Garnet

Garnet in granodiorite dikes is found only within plagioclase-dominant coronas. Grains are strongly zoned (Table 5), and two distinctive patterns have been observed: 1) simple growth-induced zoning, with a decreasing content of Mn and Ca, and an increasing content of Fe and Mg, or 2) complex zoning. Complex zoning appears to be restricted to samples with large grains of garnet that are surrounded by a cluster of smaller grains. No correlation between garnet zoning and dike composition has been found; however, there are too few data to be confident that there is no correlation.

The garnet in sample SP45a provides an example of simple zoning (Fig. 6). Grains are strongly zoned from core to rim, with the proportion of almandine and pyrope components increasing from 70 to 81, and 7 to 10 mol.%, respectively. The proportion of spessartine and grossular decrease from core to rim, 10 to 2 and 14 to 8 mol.%, respectively. No near-rim reversals are present (*e.g.*, no spessartine increase). The pattern of increasing proportion of almandine and pyrope components, and decreasing proportion of spessartine component, similar to that found in prograde pelitic garnet (Hollister 1966), is interpreted as metamorphic growth-induced zoning without significant resorption or re-equilibration.

Garnet in sample 02NC213a provides an example of complex zoning (Fig. 7). Large zoned central grains are surrounded by a halo of smaller grains with weak zoning. In their core, the central grains have sharp peaks of high almandine and spessartine, and low grossular. The core of garnet grains is surrounded by a weakly zoned mantle of decreasing pyrope and almandine, and high, nearly uniform concentrations of grossular. Smaller grains clustered around the central grain have lower almandine, pyrope, and grossular, and markedly higher spessartine concentrations, than the central grains. These grain clusters are weakly zoned radially outward from the central grain with increasing almandine, decreasing grossular and spessartine, and little or no variation in pyrope components.

Plagioclase

Plagioclase grains in most corona samples have a nearly uniform composition within each sample. However, average anorthite content varies from *ca.* An_{20} (02NC213a) to *ca.* An_{40} (98NC50) (Table 6). Many samples (*e.g.*, SP45a) contain two distinct types of plagioclase. The plagioclase in the coronas and in the matrix of this sample is mostly anhedral and unzoned (*ca.* An_{40}). However, numerous grains include a small (50–500 μm) high-Ca ($An_{60–70}$) core with oscillatory zoning (Fig. 8). Such cores are interpreted as relict igneous grains, and the weakly zoned to unzoned plagioclase grains and overgrowths are interpreted to be metamorphic.

Biotite

Biotite has a uniform composition throughout each of the rocks and shows limited variation between samples (Table 7). The ratio Fe/(Mg + Fe) varies from 0.56 to 0.73, and Ti content varies from 1.69 to 2.26% TiO_2. Biotite compositions adjacent to coronas are chemically indistinguishable from biotite in the matrix far from coronas. This lack of chemical variation is compatible with equilibrium or near-equilibrium for biotite throughout the thin sections and samples.

Phase-Equilibrium Modeling of Corona Development

Assemblages of stable minerals and chemical reactions for garnet growth and development of plagioclase-dominant corona were modeled for sample SP45a (Lake Augusta). A pressure–temperature pseudosection showing assemblages of stable minerals, and compositions and modes of selected minerals, were modeled from the bulk rock (Fig. 9). This pseudosection shows that garnet is stable over a broad range of pressure and temperature above 400ºC at 5 kbar and 450ºC at 2 kbar, and that plagioclase, quartz, and biotite are stable throughout the range investigated in the model. The peak mineral assemblage (Grt + Bt + Pl + Qtz + H_2O) is stable from 2 to 7 kbar and from 500 to almost 700ºC. The low-temperature limit of the peak assemblage is formed by addition of chlorite along the zero line in terms of chlorite mode. The high-temperature limit of this assemblage is formed by production of melt along the zero line in terms of the melt mode.

Isopleths plotted for the core of garnet grains on a pressure–temperature pseudosection can provide an estimate for initial conditions of garnet growth (Vance & Mahar 1998, Stowell *et al.* 2001). Compositional isopleths for SP45a garnet do not intersect in a point (Fig. 9a); however, the area extending between intersections of the spessartine and Fe/(Fe + Mg) isopleths with the grossular isopleth provide an initial estimate of garnet growth of 540–575ºC at 5.3–6.5 kbar. Within the field of the peak mineral assemblage, garnet mode isopleths vary from 4 to 4.5% and are widely spaced, with a moderate positive slope. Therefore, little or no growth of garnet could have occurred during equilibrium among the minerals observed in the rock. The 1% to 4.5% isopleths of garnet mode are closely spaced parallel to and at a lower temperature than the zero line in terms of the chlorite mode, which has a steep P–T slope and forms the low-temperature boundary of the field of the peak mineral assemblage, which predicts significant growth of garnet during consumption of chlorite. The 5% to 10% isopleths in garnet-mode isopleths are closely spaced parallel to and above the solidus, which predicts significant growth of peritectic garnet (see inset, Fig. 9b).

Quartz–plagioclase corona textures around garnet and predicted modes of garnet (Fig. 9b) are compatible with growth during partial melting, just above the solidus, or during solid-state reactions at temperatures below the stability of the peak assemblage of minerals. The extremely limited variation in garnet mode, 4 to <5%, within the peak mineral-assemblage field precludes significant growth of garnet in this assemblage. Peritectic growth is an unlikely explanation for all garnet because melting would be unlikely to produce the prograde zoning seen in garnet from SP45a and the central garnet from 02NC213a. Instead, closely spaced mode isopleths are compatible with garnet growth during increasing temperature in the Grt + Bt + Chl + Pl + Qtz + H_2O or Grt + Bt + Chl + Ms + Pl + Qtz + H_2O fields (Fig. 9). Garnet would have essentially ceased

a

b

FIG. 4. Dike containing plagioclase-dominant coronas on garnet, Chatter Creek campground (CC) on Icicle Creek (Fig. 2).

TABLE 2. SAMPLE LOCATIONS AND MINERALOGY OF GRANODIORITE DIKES CONTAINING PLAGIOCLASE-ON-GARNET CORONAS, NORTH CASCADES, WASHINGTON

Sample	Latitude	Longitude	Mineralogy
Lake Augusta			
SP45a	47° 39.077' N	120° 50.018' W	Qtz, Pl, Aln, Bt, Grt, Chl, Zrn, Ilm, Ap
MS54	47° 39.884' N	120° 49.410' W	Qtz, Pl, Aln, Bt, Grt, Chl, Zrn, Ilm, Ap
Top Lake			
96NC21b	47° 52.709' N	121° 9.649' W	Qtz, Pl, Aln, Bt, Grt, Chl, Zrn, Ilm, Ap
Larch Lake			
98NC50	47° 43.029' N	120° 54.433' W	Qtz, Pl, Aln, Bt, Grt, Chl, Zrn, Ilm, Ap
Heather Lake			
98NC57	47° 51.537' N	121° 7.444' W	Qtz, Pl, Bt, Grt, Chl, Zrn, Ilm, Ap
Icicle Creek			
02NC213a	47° 37.680' N	120° 57.756' W	Qtz, Sil, Pl, Ms, Bt, Grt, Chl, Zrn, Ilm, Ap

TABLE 3. REPRESENTATIVE WHOLE-ROCK COMPOSITIONS OF DIKES WITH PLAGIOCLASE-DOMINANT CORONAS AROUND GARNET, NORTH CASCADES, WASHINGTON

Sample	SP45a	02NC 213a	Normative constituents	SP45a	02NC 213a
SiO_2 wt.%	63.15	67.83	Qtz vol.%	20.40	24.15
Al_2O_3	17.29	17.78	Or	8.98	9.10
Fe_2O_3	6.00	4.00	Ab	33.09	42.22
MgO	1.44	0.68	An	20.29	12.80
MnO	0.11	0.12	Pl	An_{38}	An_{23}
CaO	4.09	2.58	Crn	1.78	3.21
Na_2O	3.91	4.99	Opx	10.78	6.57
K_2O	1.52	1.54	Mgt	1.19	0.91
TiO_2	0.55	0.25	Ilm	1.04	0.47
LOI	0.71	--			
Total	99.08	99.76	Total	97.6	99.4

LOI: loss on ignition. CIPW normative constituents: Qtz: quartz, Or: orthoclase, Ab: albite An: anorthite, Pl: plagioclase composition, Crn: corundum, Opx: orthopyroxene, Mgt: magnetite, Ilm: ilmenite.

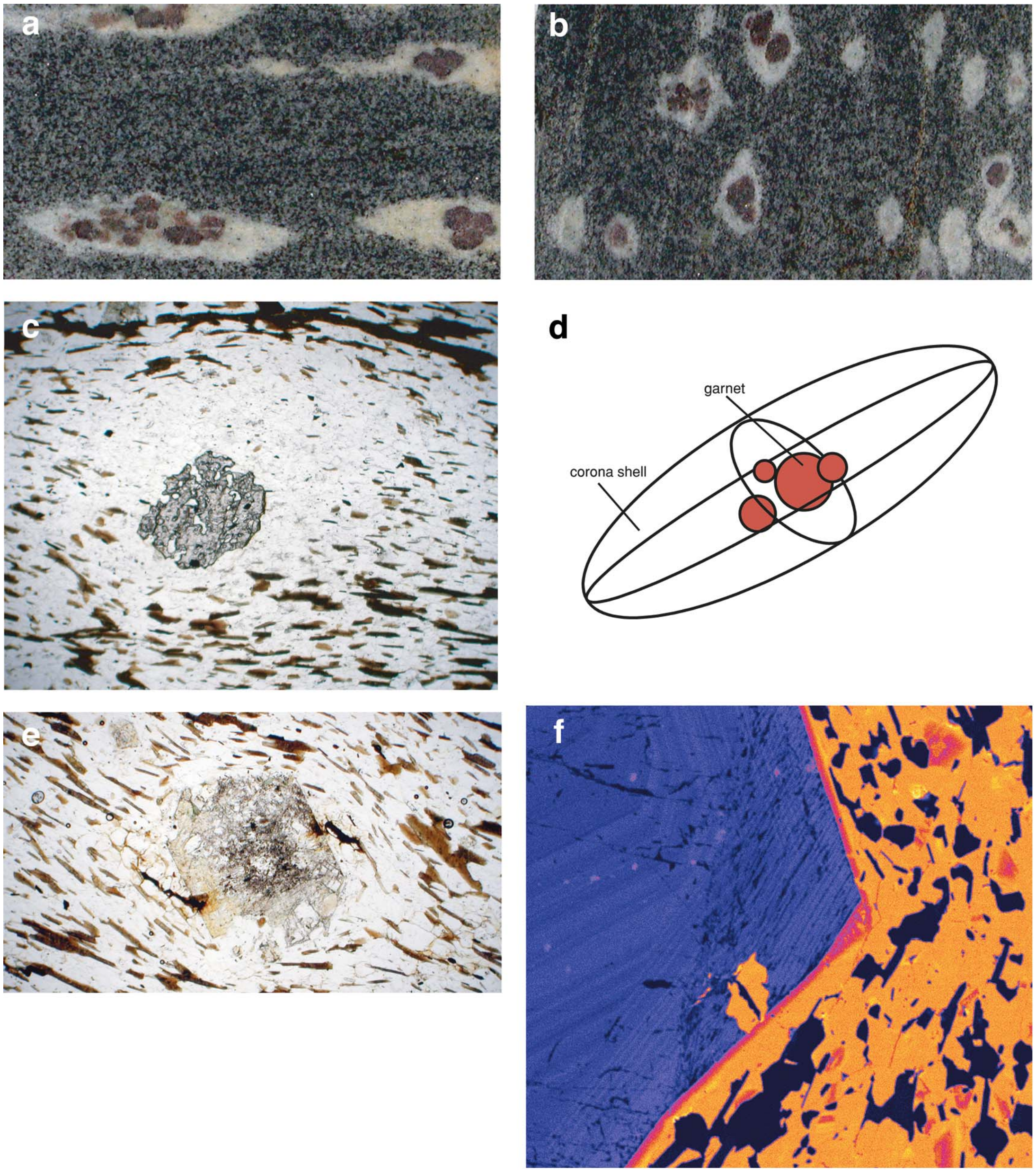

FIG. 5. Sample SP45a, granodiorite dike from near Lake Augusta (Fig. 3). a. Photograph of hand sample cut parallel to the yz plane showing plagioclase-dominant coronas on garnet. The x-dimension is *ca.* 45 mm b. Photograph of hand sample cut parallel to the xy plane showing plagioclase-dominant coronas on garnet. X dimension is *ca.* 45 mm. c. Photomicrograph of biotite foliation wrapping around a corona. X dimension is *ca.* 1.5 mm. d. Idealized ellipsoid model for "plagioclase on garnet" coronas. e. Relict phenocryst of plagioclase in plane-polarized light. Phenocryst is about 8 mm long. f. Enhanced back-scattered electron image of oscillatory zoning in relict plagioclase. X dimension is *ca.* 1 mm.

growth with consumption of all chlorite as the rock entered the field of the peak assemblage of minerals. Minor chlorite adjacent to garnet in a few samples is inferred to have replaced garnet during retrograde metamorphism.

Pressure and Temperature During Corona Development

The temperature and pressure of garnet growth and corona development can be estimated from the mineral assemblages, P–T pseudosection, and thermobarometry. However, the nature of coronas implies partial completion of mineral reactions; therefore, the extent of equilibrium must be evaluated carefully. Four samples were chosen for thermobarometry: SP45a, MS54, 98NC50, and 02NC213a. All of these samples contain quartz, plagioclase, garnet and biotite. Sample 02NC213a also contains coarse randomly oriented muscovite clustered around garnet and local mats of fibrolitic sillimanite. Biotite and plagioclase compositions were determined throughout matrix and corona assemblages in order to determine if there are chemical gradients in the samples. Uniform composition throughout the matrix indicates that equilibrium was likely attained in biotite. In addition, uniform compositions of plagioclase are found around the periphery of grains in the matrix and corona shells. These peripheral areas around relict grains and broad areas across new grains are essentially unzoned; therefore, it is reasonable to assume that all but the relict oscillatory grains were in equilibrium. Garnet generally has strong concentric zoning with uniform compositions of the rim developed around grains. The lack of chemical variation in biotite, "new" plagioclase, and garnet rims are compatible with equilibrium. Isopleths of the core composition of garnet on the pressure–temperature pseudosection for SP45a constrain initial conditions of garnet growth to 545–575°C at 5.0–6.5 kbar (Fig. 9).

TABLE 4. DIMENSIONS OF PLAGIOCLASE-DOMINANT CORONAS ON GARNET IN GRANODIORITE DIKE SP45A, LAKE AUGUSTA AREA, NORTH CASCADES, WASHINGTON

Ellipsoid axes	*x*	*y*	*z*			
Aspect ratio	1	1.8	3.07			
Volume %						
Corona	12%					
Grt subdomain		14%	80% Grt 20% Qtz	67% rim	23% inter	10% core
Shell subdomain		86%	47% Qtz 53% Pl	4% An_{60}	96% An_{40}	
Matrix	88%		13% Bt 41% Qtz 46% Pl	4% An_{60}	96% An_{40}	

The pressure estimate is clearly higher than most estimates for andalusite stability (*e.g.,* Pattison 1992), and therefore M_2 metamorphism, but equal to M_3 pressure estimates (Stowell & Tinkham 2003). Garnet + biotite equilibria were used to calculate temperatures of 595 ± 50°C for SP45a and 630 ± 50°C for MS54 from Lake Augusta, and 580 ± 50°C for 98NC50 from Larch Lake (Table 8, Fig. 3). All of these temperatures were calculated for 6 kbar on the basis of pressure estimates from the SP45a pseudosection and prior publications (Stowell & Tinkham 2003, Brown & Walker 1993). Garnet + sillimanite + plagioclase + quartz equilibria were used to calculate metamorphic conditions of 685 ± 50°C at 4.7 ± 1 kbar for sample 02NC213a from Icicle Creek (Table 8). This temperature estimate is identical to the result presented in Paterson *et al.* (1994) for this part of Icicle Creek. However, the pressure estimate is higher but within uncertainty values of results in Brown & Walker (1993).

Discussion

Timing and conditions of dike emplacement

No isotope data are available to constrain the timing of emplacement of the granodiorite dikes; therefore, only the relative timing of intrusion can be determined. Although most corona-bearing dikes described here are found adjacent to plutons (*e.g.,* the Mount Stuart batholith), they are common elsewhere, and no definite link has been made to these plutons. The relative timing of emplacement can be determined from deformed coronas and the assemblages of metamorphic minerals. Many localities, including outcrops along Icicle Creek and those at Heather and Larch lakes, contain dikes that cut straight across the folded Chiwaukum Schist. Coronas found in dikes along Icicle Creek typically show no evidence of strain; however, coronas from Larch Lake and Lake Augusta (Fig. 3) are deformed into elongate ellipsoids (*e.g.*, Fig. 5), with long axes that lie parallel to the dike boundaries. The assemblages of metamorphic minerals in dikes of almandine-rich garnet + biotite + plagioclase + quartz ± chlorite are compatible with conditions of amphibolite-facies metamorphism. Thermometry provides temperature and pressure estimates of 580–630°C and 685 ± 50°C at 4.7 ± 1 kbar for north of the Mount Stuart batholith and the septum within the batholith, respectively (Table 8, Fig. 3). Temperature estimates for SP45a, MS54, and 98NC50 are similar to peak M_3 estimates of metamorphic temperature, about 600°C, obtained for nearby samples of Chiwaukum Schist (Brown & Walker 1993, Whitney *et al.* 1999, Stowell & Tinkham 2003). The only available estimate of pressure of metamorphism of the dikes (5.0–6.5 kbar, SP45a) is indistinguishable from estimates of M_3 pressure. Therefore, dikes from Lake Augusta and presumably others are inferred to have intruded prior to or synchronous with peak M_3 metamorphism. P–T results for 02NC213a from the Icicle Creek area cannot be definitively assigned to M_2 as opposed to M_3 because this area contains no evidence for kyanite and higher-pressure metamorphism characteristic of the M_3 event north of the Mount Stuart. However, high temperatures in this part of the Chiwaukum Schist have been attributed to M_2 contact metamorphism during intrusion of the batholith. In this case, the dikes must be of equal or greater age than the Mount Stuart batholith.

Garnet growth and origin of corona textures

Garnet modes estimated from phase-equilibrium modeling clearly indicate that garnet must have grown during increasing temperature (Fig. 9). Predicted modes for chlorite and biotite, mineral textures, and garnet compositions constrain the likely reactions leading to garnet growth and possible pre-corona heterogeneities. Potentially, garnet could have grown from pre-existing high-grossular garnet, from chlorite and plagioclase in the matrix, from large high-Ca plagioclase phenocrysts that reacted to lower-Ca metamorphic plagioclase and garnet, or from high-temperature metamorphism and partial melting. Therefore, the following garnet-forming reactions should be considered:

high-grossular garnet + quartz → plagioclase + low-grossular garnet, (1)

plagioclase + biotite → garnet + melt, (2)

plagioclase + biotite or chlorite + muscovite → biotite + garnet, (3a)

and

high-Ca plagioclase + chlorite + muscovite → biotite + low-Ca plagioclase + garnet. (3b)

All of these reactions would be driven to the right by increased temperature during prograde metamorphism; however, a dramatic decrease in grossular content in garnet [reaction (1)] would require decompression (see grossular isopleth in Fig. 9a).

A precursor garnet could have occupied the space now filled with garnet and corona minerals and reacted to garnet plus corona: reaction (1). Assuming that this

TABLE 5. REPRESENTATIVE COMPOSITIONS OF GARNET IN PLAGIOCLASE-DOMINANT CORONAS IN GRANODIORITE DIKES, NORTHERN CASCADES, WASHINGTON

Sample	SP45a core	SP45a rim	MS54 rim	02NC213a core	02NC213a rim
SiO_2 wt.%	36.42	36.35	36.73	37.37	37.97
Al_2O_3	20.93	21.06	21.14	20.90	21.12
FeO	31.37	35.03	36.20	34.38	34.55
MgO	1.79	2.32	2.42	2.16	1.81
MnO	3.86	0.75	0.71	4.25	5.67
CaO	4.17	2.78	2.76	1.66	0.72
Total	98.67	98.30	99.96	100.97	101.83
Si *apfu*	2.98	2.98	2.97	3.03	3.00
Al	2.02	2.04	2.02	1.99	1.98
Fe^{2+}	2.15	2.40	2.45	2.30	2.31
Mg	0.22	0.28	0.29	0.21	0.26
Mn	0.27	0.05	0.05	0.38	0.29
Ca	0.37	0.24	0.24	0.06	0.14
Total	8.00	8.00	8.02	7.98	7.99
Fe#	0.91	0.89	0.89	0.91	0.90
Alm	0.72	0.80	0.81	0.78	0.77
Prp	0.07	0.09	0.10	0.07	0.09
Sps	0.09	0.02	0.02	0.13	0.10
Grs	0.12	0.08	0.08	0.02	0.05

Fe# = Fe/(Fe + Mg), n.a. = not analyzed, n.c. = not calculated. Compositions are recast into atoms per formula unit (*apfu*) on the basis of 12 atoms of oxygen. Alm: mole fraction of almandine, Prp: mole fraction of pyrope, Sps: mole fraction of spessartine, Grs: mole fraction of grossular.

TABLE 6. REPRESENTATIVE COMPOSITIONS OF PLAGIOCLASE IN CORONAS AROUND GARNET IN GRANODIORITE DIKES, NORTHERN CASCADES, WASHINGTON

Sample Pt#	SP45a 67	SP45a 5	MS54 2	02NC213a 177	98NC50 2
SiO_2 wt.%	45.53	55.64	57.54	61.74	55.94
Al_2O_3	34.30	27.65	27.84	23.70	28.25
CaO	16.66	8.28	8.26	4.06	8.80
Na_2O	1.73	6.73	6.71	9.17	6.08
K_2O	0.01	0.03	0.06	0.07	0.08
Total	98.24	98.38	100.50	98.77	99.25
Si *apfu*	2.13	2.53	2.56	2.76	2.52
Al	1.89	1.48	1.46	1.25	1.50
Ca	0.83	0.40	0.39	0.19	0.43
Na	0.16	0.59	0.58	0.80	0.53
K	0.00	0.00	0.00	0.00	0.00
Total	5.01	5.02	5.00	5.01	4.99
An	0.84	0.40	0.40	0.20	0.44
Ab	0.16	0.59	0.59	0.80	0.55

An: mole fraction of anorthite, Ab: mole fraction of albite. Compositions are recast into atoms per formula unit (*apfu*) on the basis of 8 atoms of oxygen

TABLE 7. REPRESENTATIVE COMPOSITIONS OF BIOTITE ADJACENT TO PLAGIOCLASE-DOMINANT CORONAS ON GARNET IN GRANODIORITE DIKES, NORTHERN CASCADES, WASHINGTON

Sample Pt#	SP45a 83	MS54 67	02NC213a 36	98NC50 6
SiO_2 wt.%	34.85	35.15	33.49	35.65
TiO_2	1.82	1.86	2.26	1.69
Al_2O_3	19.66	19.29	20.18	20.68
FeO	20.25	22.16	25.52	20.39
MnO	0.04	0.04	0.20	0.10
MgO	8.36	8.68	5.41	8.91
Na_2O	0.08	0.10	0.07	0.26
K_2O	9.49	9.08	9.27	8.90
Total	94.55	96.36	96.40	96.58
Si *apfu*	5.49	5.35	5.20	5.34
Ti	0.22	0.21	0.26	0.19
Al	3.65	3.46	3.69	3.65
Fe	2.67	2.82	3.32	2.56
Mn	0.00	0.00	0.03	0.01
Mg	1.96	1.97	1.25	1.99
Na	0.01	0.03	0.02	0.08
K	0.95	1.76	1.84	1.70
Fe#	0.58	0.59	0.73	0.56

Compositions are recast into atoms per formula unit (*apfu*) on the basis of 22 atoms of oxygen.

high-grossular (Grs *ca.* 45%) garnet incorporated all of the available Fe, Mn, Mg, and Ca in the corona, there would have been excess Al. Ca or other divalent cation mobility could have allowed this excess Al to have been incorporated into garnet. For example, if Ca was mobile and Al was immobile, a precursor garnet that utilized all Al in the corona would have had a grossular mole fraction of *ca.* 79%. Reaction (1) seems highly unlikely because no relict high-grossular garnet has been found, relict pre-metamorphic plagioclase grains with high Ca (see above) are common within coronas, suggesting more extensive pre-metamorphic plagioclase, not larger grains of garnet that predate the coronas, and metamorphic plagioclase is clearly lower in Ca and cannot have provided a sink for calcium released from grossular breakdown.

Growth of peritectic garnet during partial melting could produce a corona of locally produced melt around garnet porphyroblasts according to reaction (2). Well-developed "prograde" zoning in garnet SP45a, lack of igneous textures (*e.g.,* triple junctions among grains) in the coronas, and preservation of pre-metamorphic plagioclase in the coronas make this scenario unlikely as an explanation for all of the garnet. However, produc-

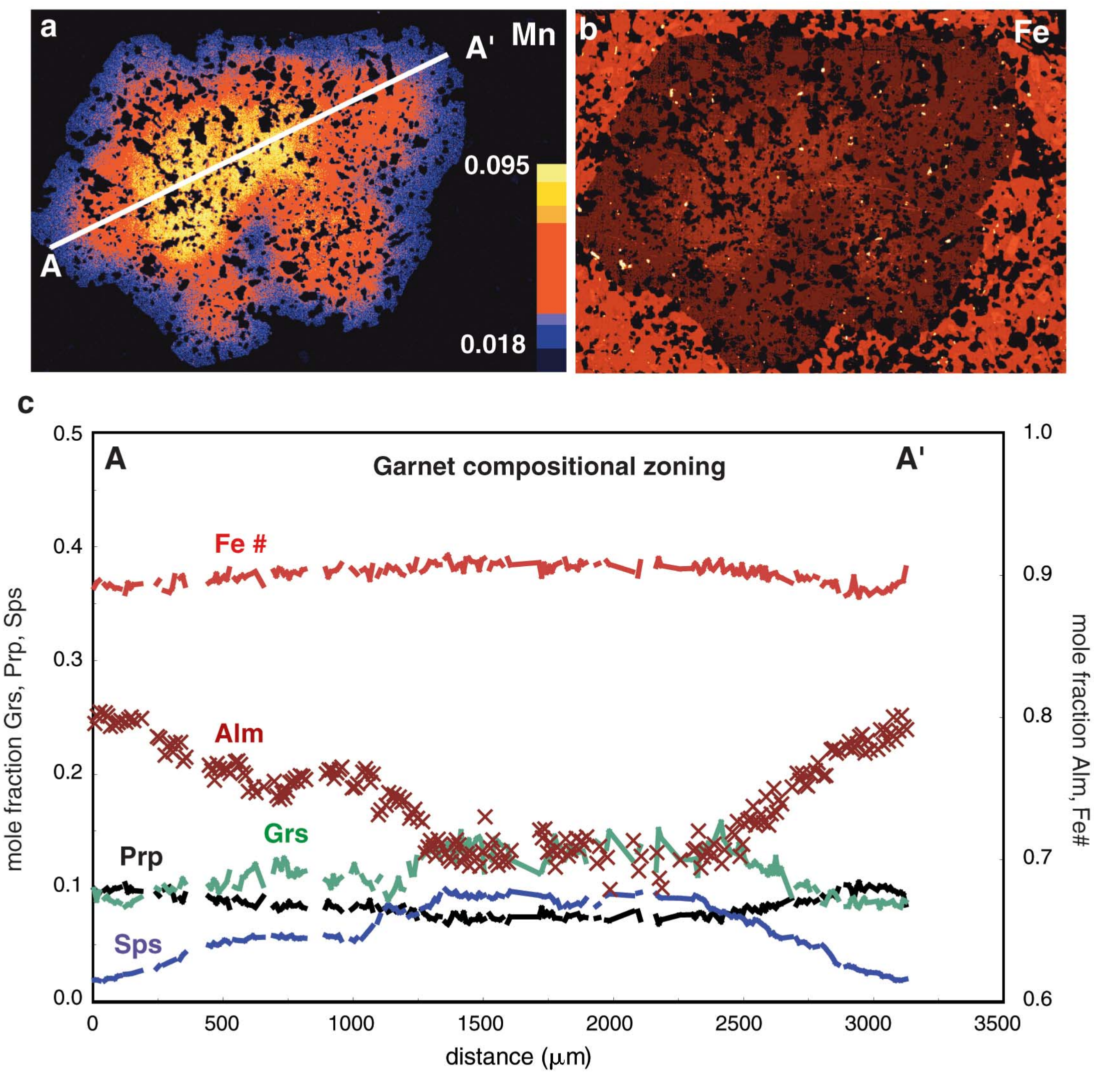

FIG. 6. Garnet zoning in sample SP45a granodiorite dike from near Lake Augusta, Washington (Fig. 3). a. Mn*K*α X-ray map. b. Fe*K*α X-ray map. c. Mole fraction of almandine, grossular, pyrope, and spessartine along line A–A' shown in Figure 6a.

tion of some garnet during partial melting that consumed biotite in the corona is plausible. Preliminary thermodynamic modeling on sample 02NC213a suggests that garnet grains in the outer cluster (Fig. 7) may have formed during partial melting. This interpretation is supported by increases in garnet mode above the solidus and an estimated metamorphic temperature of 685°C for 02NC213a, which is *ca.* 50°C above the solidus temperature estimated from a preliminary analysis of pseudosections (E. Stein, unpubl. data).

Reaction of plagioclase with biotite or chlorite could have produced garnet: reaction (3a). Pseudosection modeling clearly indicates that plagioclase and biotite modes increase with temperature, muscovite and chlorite modes decrease with temperature, and equilibrium compositions of plagioclase are the same as those in the rock ($An_{35–40}$). In addition, increases in garnet mode are clearly associated with decreases in chlorite mode. Therefore, early high-Ca plagioclase must have reacted during metamorphism to produce lower-Ca plagioclase. This reaction would provide Al and Ca for garnet growth according to reaction (3b). The presence of relict high-Ca plagioclase in the coronas and matrix suggests that plagioclase in the precursor assemblage was more calcium-rich than the bulk of the plagioclase in the observed assemblage, making less Ca available before growth of the observed garnet. Therefore, growth of garnet from an assemblage containing high-Ca plagioclase and biotite or chlorite is plausible. In this scenario, garnet growth would have been accompanied by growth of new lower-Ca plagioclase. Growth of the existing garnet from a mineral assemblage resembling the matrix (biotite + plagioclase + quartz) would provide the necessary elements for growth of garnet and the corona. However, the P–T pseudosection predicts that garnet mode would only increase significantly in mineral assemblages that include chlorite or melt (Fig. 9) and that biotite mode increases with garnet in the field of the peak mineral-assemblage. Therefore, chlorite is the most likely source of Fe, Mg, and possibly Al for growth of garnet.

Corona textures involving plagioclase on garnet in granodiorite dikes described here are of two distinct types: those cored by garnet with simple zoning, and those cored by garnet with complex zoning. Therefore, the corona textures may have developed by more than one mechanism. Those coronas that are cored by simply zoned garnet (*e.g.*, SP45a) are interpreted to have developed during prograde growth of garnet from chlorite and plagioclase, according to reaction (3b). Those coronas that are cored by complexly zoned garnet (*e.g.*, 02NC213a) may have developed in a two-stage fash-

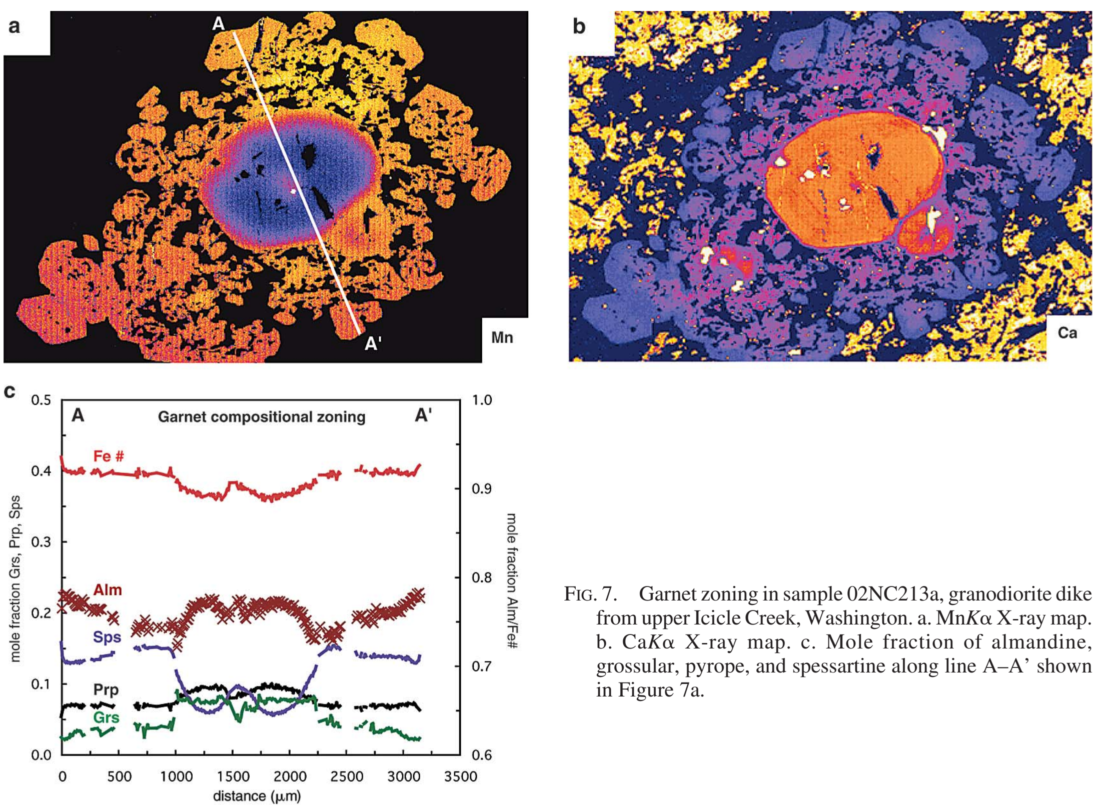

FIG. 7. Garnet zoning in sample 02NC213a, granodiorite dike from upper Icicle Creek, Washington. a. Mn$K\alpha$ X-ray map. b. Ca$K\alpha$ X-ray map. c. Mole fraction of almandine, grossular, pyrope, and spessartine along line A–A' shown in Figure 7a.

ion. Early garnet in the center of coronas may have formed by similar prograde metamorphic reactions as those inferred for SP45a. Later grains of garnet, rimming the central garnet, may have formed by partial melting as temperature exceeded the solidus or by a two-stage process of igneous crystallization followed by metamorphic overgrowth.

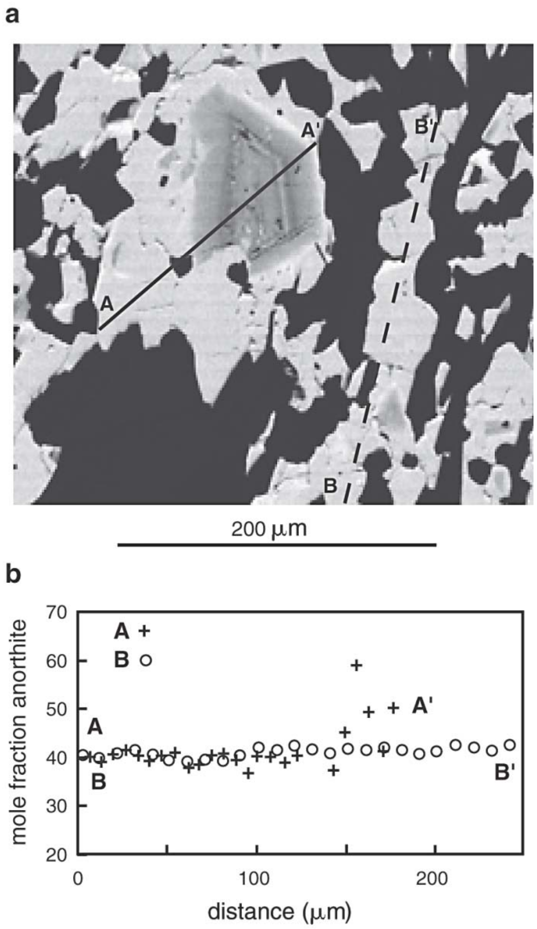

FIG. 8. Plagioclase zoning in sample SP45a, granodiorite dike from near Lake Augusta, Washington. a. Na X-ray map of plagioclase grains in the matrix. Dark gray oscillatory-zoned areas are calcic ($An_{60–70}$) and are interpreted as relict phenocrysts. Light gray anhedral unzoned areas are less calcic (An_{40}) and are interpreted as metamorphic overgrowths. Large cores, such as the one at center, which is *ca.* 1 mm across, are rare, but smaller ones, as in the lower portion of the image, are very common throughout both the matrix subdomains and the shell subdomain of the coronas, accounting for approximately 4% of all plagioclase. Black areas in the image are quartz grains. Modal ratio of quartz to plagioclase is 0.89. b. The anorthite content of plagioclase along lines A–A' and B–B', shown in Figure 8a.

Plagioclase-dominant coronas on garnet with simple zoning (*e.g.*, SP45a) are interpreted as Fe–Mg depletion halos that developed during prograde growth of garnet. Garnet grains show concentric zoning that is compatible with prograde growth with little or no subsequent modification. The coronas are devoid of biotite and contain plagioclase that is dominantly unzoned, with low- to medium-An contents identical to those found in matrix plagioclase; however, small grains of high-Ca plagioclase within the lower-Ca plagioclase have oscillatory zoning and likely represent relict igneous grains. Coronas likely developed by consumption of chlorite and high-Ca plagioclase in the vicinity of the growing grains of garnet. Cessation of garnet growth may have been related to complete consumption of chlorite, declining temperature and diffusion rates, increased distances required for intergranular diffusion of cations to the growing grain, or to near-total depletion of Mn in the matrix, leading to decreased stability of the garnet. Initial growth of garnet likely took place during M_3 metamorphism, which is estimated to have reached temperatures of *ca.* 600ºC. If dikes intruded prior to emplacement of the Mount Stuart batholith or during an early phase of the batholith, then all garnet growth could be M_2. However, pressure estimates of *ca.* 6 kbar from the SP45a pseudosection modeling are higher than pressure estimates for andalusite-zone contact metamorphism and are most compatible with M_3 growth.

Plagioclase-dominant coronas on garnet with complex zoning (*e.g.*, 02NC213a) likely formed by initial growth of metamorphic garnet from chlorite, followed by additional growth during partial melting. The central grains could have an igneous origin; however, the sharp decreases in Mn concentration near the center of grains is atypical of garnet in high-temperature equilibrium with a magma. Subsequent metamorphism, above the solidus, presumably resulted in growth of new garnet in a cluster of smaller crystals. High concentrations of Mn in the outer cluster of garnet (Fig. 7) are compatible with a new source of Mn during late growth of garnet. Lack

TABLE 8. TEMPERATURE AND PRESSURE ESTIMATES OF METAMORPHISM OF GRANODIORITE DIKES, NORTHERN CASCADES, WASHINGTON

Sample	Temperature (°C)	Pressure (kbar)	Method	Reference
Lake Augusta				
SP45a	595	5-6[1]		Ferry & Spear (1978)
MS54	630	6[2]		Ferry & Spear (1978)
Larch Lake				
98NC50	580	6[2]		Ferry & Spear (1978)
Icicle Creek				
02NC213a	685		Grt-Bt	Ferry & Spear (1978)
		4.7	Grt-Sil-Pl-Qtz	Newton & Haselton (1981)
				Koziol & Newton (1988)

[1] Pressure determined from garnet core compositions and pseudosection in Figure 9.
[2] Pressure assumed from the results of Stowell & Tinkham (2003), and Brown & Walker (1993).
Uncertainties are taken as ±50°C and ±1 kbar, for temperature and pressure, respectively. Activity models are from Hodges & Spear (1982).

of Mn-bearing ilmenite grains in the matrix is compatible with breakdown of ilmenite during late growth of garnet. However, Mn could also have been supplied by breakdown of biotite during partial melting. Initial growth of garnet likely occurred during M_2 metamorphism. An alternative interpretation is that the initial garnet in the center of the clusters is igneous, and later metamorphism and partial melting resulted in growth of new garnet in a cluster of smaller grains. In both cases, the overgrowth of smaller grains of garnet may have been facilitated by nucleation on the pre-existing central grain. Plagioclase-dominant coronas are inferred to have developed by depletion of Fe and Mg during growth of the late clusters of garnet in the same manner as coronas on simply zoned garnet. Second-stage peritectic garnet could have grown during M_2 contact metamorphism, even if the dikes and early garnet are synchronous with the Mount Stuart batholith, because intrusive ages for plutons in the batholith range from 96 to 91 Ma, on the basis of U–Pb dates obtained on zircon. Late clusters of garnet grains could also have grown during M_3 regional metamorphism; however, there are no published data supporting M_3 garnet-zone metamorphism along Icicle Creek.

Tectonic implications

The data described herein are most compatible with development of corona textures in the granodiorite dikes during prograde metamorphism. In this case, the texture cannot be used to infer high-temperature decompression of the Nason terrane because garnet simply ceased to grow owing to declining temperature or lack of reactants nearby. However, the similarity of textures over a wide area of the southern Wenatchee block is compatible with similar processes causing the plagioclase-dominant coronas. It is likely that limited distances of intergranular diffusion, perhaps caused by rapid cooling or low availability of fluid, was common during the latter stages of metamorphism. Rapid cooling and low availability of fluid may have played roles in corona development, given the thermochronological data for rapid cooling shortly after metamorphism (Paterson *et al.* 1994, Whitney *et al.* 1999, Evans & Davidson 1999) and the likely low content of fluid in the granodiorite dikes. The assumption that the dikes are associated with emplacement of the Mount Stuart batholith and that garnet and the coronas grew during subsequent metamorphism requires that M_3 metamorphism reached temperatures of *ca.* 685ºC at Icicle Creek, and *ca.* 595 and 630ºC at Lake Augusta and Larch Lake, respectively. Most importantly, conditions of growth of the garnet core for sample SP45a constrain metamorphic pressures to greater than 5 kbar, most compatible with the loading event that caused M_3 metamorphism. Therefore, garnet is inferred to have grown synchronously with corona development after intrusion of the Mount Stuart batholith and during prograde M_3 metamorphism.

Conclusions

Plagioclase-dominant coronas on garnet in granodiorite dikes adjacent to the Mount Stuart batholith are interpreted to have developed during prograde amphibolite-facies M_3 metamorphism. This interpretation, based on garnet textures, compositional zoning in garnet and plagioclase, and forward thermodynamic modeling, requires that dikes intruded prior to the last metamorphic event. However, no geochronological data are available at this time. In addition, elongate coronas of recrystallized plagioclase and quartz in dike samples from Lake Augusta clearly indicate that significant deformation postdated emplacement and was likely nearly synchronous with metamorphism.

The widespread development of corona textures in granodiorite dikes is compatible with similar metamorphic processes throughout the southern Wenatchee block. Processes that likely played a role in development of the texture are: consumption of chlorite and depletion of Fe and Mg adjacent to growing porphyroblasts of garnet, incomplete reaction of pre-existing high-Ca plagioclase during garnet growth, and limited distances of intergranular diffusion. Diffusion distances were likely limited by temperature because rapid cooling occurred over a wide area of the Cascades Core soon after metamorphism (Whitney *et al.* 1999, Evans & Davidson 1999).

Acknowledgements

Development of the ideas presented here about metamorphic pressure – temperature – time paths benefitted from the insightful work on bathograds completed by Dugald Carmichael. Research would not have been possible without support to E. Stein from the Geological Society of America, the Graduate School of the University of Alabama, the Hooks Fund of the Department of Geological Sciences, University of Alabama, and the Alabama Graduate Student Association. Additional funding was provided by National Science Foundation grants EAR–0207777 (H. Stowell) and EAR–9628232 (purchase of X-ray fluorescence spectrometer). Samples SP45a and MS54 were kindly provided by S. Paterson. The authors thank B. Evans, R. Miller, S. Paterson, H. Stein, D. Tinkham, and C. Zuluaga for discussions and field assistance. This manuscript benefitted from helpful reviews by A. Indares, J. Percival, and M.R. St-Onge.

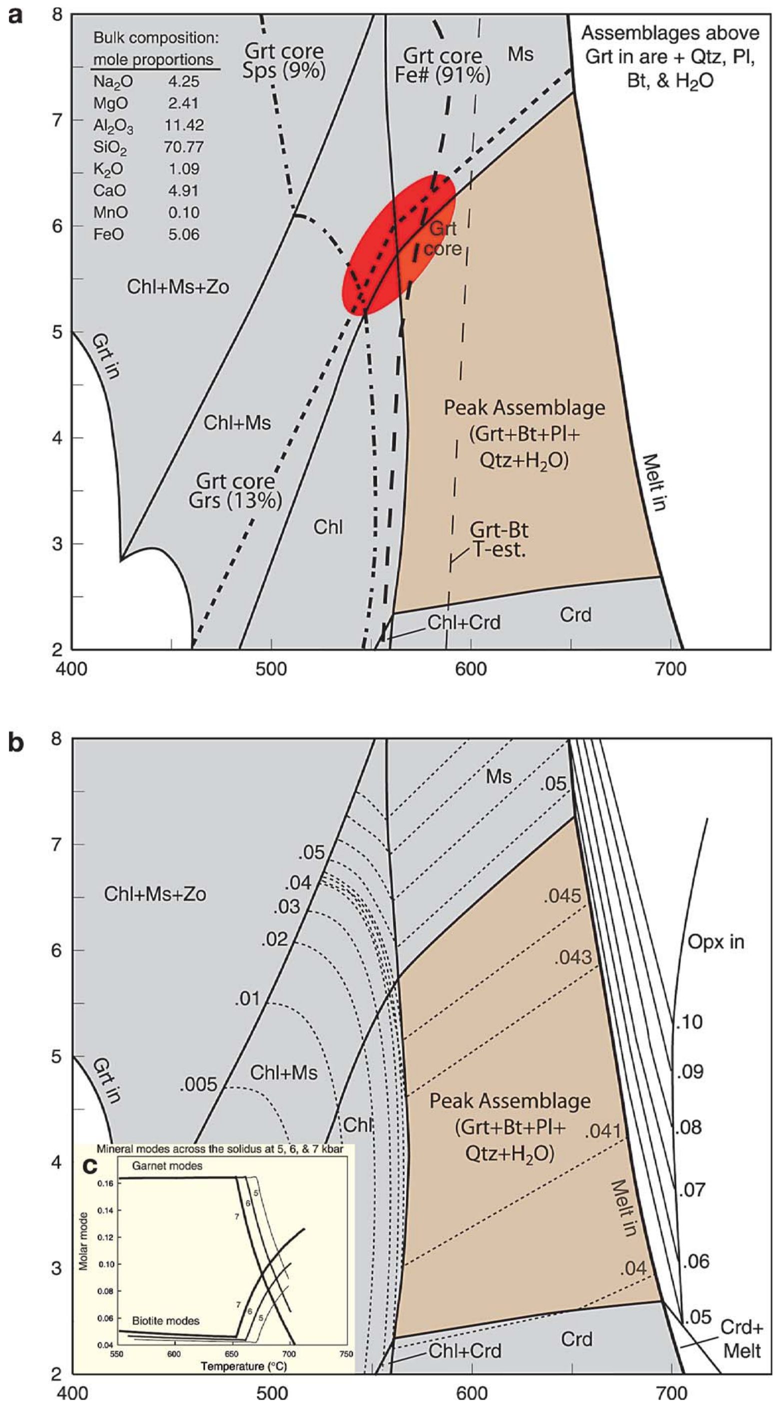

FIG. 9. Pressure–temperature pseudosections for sample SP45a, constructed for the bulk composition of the dike in Table 3. All equilibria were calculated with H_2O in excess. a. Predicted equilibrium mineral assemblages and isopleths for core compositions of the garnet [Fe/(Fe + Mg), spessartine, grossular]. b. Garnet modes (molar) plotted on the same pseudosection as shown in Figure 9a. Model lines are dashed below the solidus and solid above the solidus. c. Inset of garnet and biotite modes between 550 and 750ºC along 5, 6, and 7 kbar isobars.

REFERENCES

ARMSTRONG, J.T. (1984): Quantitative analysis of silicate and oxide minerals: a re-evaluation of ZAF corrections and proposal for new Bence–Albee coefficients. *Microbeam Anal.*, 208.

BARKER, A.J. (1990): *Introduction to Metamorphic Textures and Microstructures*. Blackie, Glasgow, U.K.

BROWN, E.H. & WALKER, N.W. (1993): A magma loading model for Barrovian metamorphism in the SE Coast Plutonic Complex, British Columbia and Washington. *Geol. Soc. Am., Bull.* **105**, 479-500.

CHACE, R.J., STOWELL, H.H. & TINKHAM, D.K. (1998): The timing and conditions of high pressure metamorphism in the Nason Terrane, Cascades Crystalline Core, WA. *Geol. Soc. Am., Abstr. Programs* **30**(5), 9.

CONEY, P.J., JONES, D.L. & MONGER, J.W.H. (1980): Cordilleran suspect terranes. *Nature* **288**, 329-333.

ENGELS, J.C., TABOR, R.W., MILLER, F.K. & OBRADOVICH, J.D. (1976): Summary of K–Ar, Rb–Sr, U–Pb, Pb-alpha, and fission-track ages for rocks from Washington State prior to 1975 (exclusive of Columbia Plateau basalts). *U.S. Geol. Surv., Map* **MF-710**.

EVANS, B.W. & BERTI, J.W. (1986): Revised metamorphic history for the Chiwaukum Schist, North Cascades, Washington. *Geology* **14**, 695-698.

________ & DAVIDSON, G.F. (1999): Kinetic control of metamorphic imprint during synplutonic loading of batholiths; an example from Mount Stuart, Washington. *Geology* **27**, 415-418.

FERRY, J. & SPEAR, F.S. (1978): Experimental calibration of the partitioning of Fe and Mg between biotite and garnet. *Contrib. Mineral. Petrol.* **66**, 113-117.

HAUGERUD, R.A., BROWN, E.H., TABOR, R.W., KRIENS, B.J. & MCGRODER, M.F. (1994): Late Cretaceous and early Tertiary orogeny in the North Cascades. *In* Geologic Field Trips in the Pacific Northwest **2** (D.A. Swanson & R.A. Haugerud, eds.). Geol. Soc. Am. and Dept. of Geol. Sci., Univ. of Washington, 51 (Chapter 2E).

________, VAN DER HEYDEN, P., TABOR, R.W., STACEY, J.S. & ZARTMAN, R.E. (1991): Late Cretaceous and early Tertiary plutonism and deformation in the Skagit gneiss complex, North Cascade Range, Washington and British Columbia *Geol. Soc. Am., Bull.* **103**, 1297-1307 (with Suppl. Data 91-25).

HODGES, K.W. & SPEAR, F.S. (1982): Geothermometry, geobarometry and the Al_2SiO_5 triple point at Mt. Moosilauke, New Hampshire. *Am. Mineral.* **67**, 1118-1134.

HOLLAND, T.J.B. & POWELL, R. (1998): An internally consistent thermodynamic data set for phases of petrological interest. *J. Metamorph. Geol.* **16**, 309-343.

HOLLISTER, L.S. (1966): Garnet zoning; an interpretation based on the Rayleigh fractionation model. *Science* **154**, 1647-1651.

KOZIOL, A. & NEWTON, R. (1988): Redetermination of the anorthite breakdown reaction and improvement of the plagioclase – garnet – Al_2SiO_5 – quartz geobarometer. *Am. Mineral.* **73**, 216-223.

LONGTINE, M.W. (1991): *Mid- to Late Cretaceous Structural, Metamorphic, and Magmatic Evolution of the Sloan Peak Area, North Cascades, Washington*. M.S. thesis, Univ. of Texas, Austin, Texas.

MAGLOUGHLIN, J.F. (1993): *A Nason Terrane trilogy. I. Nature and Significance of Pseudotachylyte. II. Summary of the Structural and Tectonic History. III. Major and Trace Element Geochemistry and Strontium and Neodymium Isotope Geochemistry of the Chiwaukum Schist, Amphibolite, and Meta-Tonalite Gneiss of the Nason Terrane*. Ph.D. dissertation, Univ. Minnesota, Minneapolis, Minnesota.

MCGRODER, M.F. (1991): Reconciliation of two-sided thrusting, burial metamorphism, and diachronous uplift in the Cascades of Washington and British Columbia. *Geol. Soc. Am., Bull.* **103**, 189-209.

MILLER, R.B. (1985): The ophiolitic Ingalls Complex, north-central Cascade Mountains, Washington. *Geol. Soc. Am., Bull.* **96**, 27-42.

________, BOWRING, S.A. & HOPPE, W.J. (1989): Paleocene plutonism and its tectonic implications, North Cascades, Washington. *Geology* **17**, 846-849.

________, MATZEL, J.P., PATERSON, S.R. & STOWELL, H.H. (2003): Cretaceous to Paleocene Cascades Arc: structure, metamorphism, and timescales of magmatism, burial, and exhumation of a crustal section. *In* Western Cordillera and Adjacent Areas (T.W. Swanson, ed.). *Geol. Soc. Am., Field Guide* **4**, 107-135.

________, PATERSON, S.R., DEBARI, S.M. & WHITNEY, D.L. (2000): North Cascades Cretaceous crustal section: changing kinematics, rheology, metamorphism, pluton emplacement, and petrogenesis from 0 to 40 kilometers depth. *In* Guidebook for Geological Field Trips in Southwestern British Columbia and Northern Washington. *Geol. Soc. Am., Cordilleran Sect.*, 229-278.

MISCH, P. & ONYEAGOCHA, A.C. (1976): Symplectite breakdown of Ca-rich almandines in upper amphibolite-facies skagit gneiss, North Cascades, Washington. *Contrib. Mineral. Petrol*. **54**, 189-224.

MONGER, J.W.H., PRICE, R.A. & TEMPLEMAN-KLUIT, D.J. (1982): Tectonic accretion of the two major metamorphic and plutonic welts of the Canadian Cordillera. *Geology* **10**, 70-75.

NEWTON, R.C. & HASELTON, H.T. (1981): Thermodynamics of the garnet – plagioclase – Al_2SiO_5 – quartz geobarometer. *In* Thermodynamics of Minerals and Melts (R.C. Newton,

A. Navrotsky & B.J. Wood, eds.). Springer-Verlag, New York, N.Y. (129-145).

PATERSON, S.R. & MILLER, R.B. (1998): Magma emplacement during arc-perpendicular shortening; an example from the Cascades crystalline core, Washington. *Tectonics* **17**, 571-586.

________, ________, ANDERSON, J.L., LUND, S., BENDIXEN, J., TAYLOR, N. & FINK, T. (1994): Emplacement and evolution of the Mt. Stuart batholith. *In* Geologic Field Trips in the Pacific Northwest **2F**. *Geol. Soc. Am. and Dept. of Geol. Sci., Univ. of Washington*, 47.

PATTISON, D.R. (1992): Stability of andalusite and sillimanite and the Al_2SiO_5 triple point: constraints from the Ballachulish aureole, Scotland. *J. Geol.* **100**, 423-446.

PLUMMER, C.C. (1980): Dynamothermal contact metamorphism superposed on regional metamorphism in the pelitic rocks of the Chiwaukum Mountains area, Washington Cascades. *Geol. Soc. Am., Bull.* **91**, 386-388.

SPRY, A. (1969): *Metamorphic Textures.* Pergamon, Oxford, U.K.

STEIN, E. & STOWELL, H.H. (2002). Thermobarometric constraints on high-pressure exhumation history of the Dinkelman decollement, North Cascades, Washington: a record of decompression in amphibolite garnet coronas. *Geol. Soc. Am., Abstr. Programs.* **34**(6), 432.

STOWELL, H.H. & CRAWFORD, M.L. (2000): Metamorphic history of the western Coast plutonic-metamorphic complex, western British Columbia and southeast Alaska. *In* Tectonics of the Coast Mountains, Southeastern Alaska and British Columbia (H.H. Stowell & W.C. McClelland, eds.). *Geol. Soc. Am., Spec. Pap*. **343**, 257-283.

________, TAYLOR, D.L., TINKHAM, D.K., GOLDBERG, S.A. & OUDERKIRK, K.A. (2001): Contact metamorphic P–T–t paths from Sm–Nd garnet ages, phase equilibria modeling, and thermobarometry: Garnet Ledge, southeastern Alaska. *J. Metamorph. Geol.* **19**, 645-660.

________ & TINKHAM, D.K. (2003): Integration of phase equilibria modelling and garnet Sm–Nd chronology for construction of P–T–t paths: examples from the Cordilleran Coast Plutonic Complex, USA. *In* Geochronology: Linking the Isotopic Record with Petrology and Textures (D. Vance, W. Muller & I. Villa, eds.). *Geol. Soc., Spec. Publ.* **220**, 119-145.

TABOR, R.W., BOOTH, D.B., VANCE, J.A. & FORD, A.B. (2002): Geologic map of the Sauk River 30- by 60-minute quadrangle, Washington. *U.S. Geol. Surv., Map* **I-2592**.

________, FRIZZELL, V.A., JR., BOOTH, D.B., WAITT, R.B., WHETTEN, J.T. & ZARTMAN, R.E. (1993): Geologic map of the Skykomish River 30- by 60-minute Quadrangle, Washington. *U.S. Geol. Surv., Map* **I-1963**, 42.

________, ________, WHETTEN, J.T., WAITT, R.B., Jr., SWANSON, D.A., BYERLY, G.R., BOOTH, D.B., HETHERINGTON, M.J. & ZARTMAN, R.E. (1987): Geologic map of the Chelan 30' by 60' Quadrangle, Washington. *U.S. Geol. Surv., Map* **I-1661**, 29.

________, WAITT, R.B., Jr., FRIZZELL, V.A., Jr., SWANSON, D.A., BYERLY, G.R. & BENTLEY, R.D. (1982): Geologic map of the Wenatchee 1:100,000 Quadrangle, central Washington. *U.S. Geol. Surv., Map* **I-1311**, 26.

TINKHAM, D.K. (2002): *MnNCKFMASH Phase Equilibria, Garnet Activity Modeling, and Garnet Samarium–Neodymium Chronology: Applications to the Waterville Formation, Maine, and South-Central Nason Terrane, Washington*. Ph.D. dissertation, Univ. Alabama, Tuscaloosa, Alabama.

________, ZULUAGA, C.A. & STOWELL, H.H. (2001): Metapelite phase equilibria modeling in MnNCKFMASH: the effect of variable Al_2O_3 and MgO/(MgO + FeO) on mineral stability. *Geol. Mater. Res.* **3**(1), 1-42.

UMHOEFER, P.J. & MILLER, R.B. (1996): Mid-Cretaceous thrusting in the southern Coast Belt, British Columbia and Washington, after strike-slip fault reconstruction. *Tectonics* **15**, 545-565.

VANCE, D. & MAHAR, E. (1998): Pressure–temperature paths from P–T pseudosections and zoned garnets; potential, limitations and examples from the Zanskar Himalaya, NW India. *Contrib. Mineral. Petrol.* **132**, 225-245.

WERNICKE, B. & GETTY, S.R. (1997): Intracrustal subduction and gravity currents in the deep crust: Sm–Nd, Ar–Ar, and thermobarometric constraints from the Skagit Gneiss Complex, Washington. *Geol. Soc. Am., Bull.* **109**, 1149-1166.

WHITNEY, D.L. (1992): High-pressure metamorphism in the western Cordillera of North America: an example from the Skagit Gneiss, North Cascades, Washington. *J. Metamorph. Geol.* **10**, 71-85.

________ & MCGRODER, M.F. (1989): Cretaceous crustal section through the proposed Insular-Intermontane superterrane suture. *Geology* **17**, 555-558.

________, MILLER, R.B. & PATERSON, S.R. (1999): P–T–t evidence for mechanisms of vertical tectonic motion in a contractional orogen; north-western US and Canadian Cordillera. *J. Metamorph. Geol.* **17**, 75-90.

WINTER, J.D. (2001): *An Introduction to Igneous and Metamorphic Petrology*. Prentice Hall, Upper Saddle River, N.J.

Received October 23, 2003, revised manuscript accepted June 6. 2004.

APPENDIX: ANALYTICAL PROCEDURES

Electron-microprobe analysis

Quantitative analyses of the minerals and X-ray maps were collected with the JEOL 8600 electron-probe micro-analyzer at the University of Alabama using wavelength-dispersion spectrometry. Major-element analyses were made with a beam 1 to 5 μm in diameter at a current of 20 nA under a 15 kV accelerating potential. Trace element analyses were made with a beam 1 to 5 μm in diameter at a beam current of 50 nA under a 20 kV accelerating potential. Raw counts from characteristic X-ray peaks were converted to weight percent oxides by comparison with natural mineral and synthetic standards, using the CitZAF correction technique of Armstrong (1984). Count times ranged from 30 to 45 seconds. Operating conditions for collection of X-ray maps were accelerating potential 15 kV, beam current 75 to 300 nA, and a beam 1 μm beam in diameter. Count times ranged from 5 to 50 ms / pixel. Quantitative analyses across minerals were acquired to characterize chemical zoning. For garnet, X-ray maps were routinely acquired before quantitative analyses in order to determine where to collect data through the chemical core of garnet crystals, defined as the interior portion with the highest Mn content.

X-ray-fluorescence analysis

The whole-rock composition of SP45a, determined by X-ray fluorescence on a glass disc, was obtained commercially from Activation Laboratories Ltd. The whole-rock composition of sample 02NC213a was determined from a glass disc at the University of Alabama. Bulk-rock samples of ≥30 g were used to obtain the bulk composition. Rock chips were ground on a diamond-embedded lap to remove surfaces that were cut by the rock saw or had signs of weathering; they were washed, and rinsed in acetone and 2M HCl before jaw crushing and grinding to a powder in a steel ring-and-puck mill. Samples prepared and analyzed at the University of Alabama were mixed with several drops of saturated polyvinyl alcohol solution to enhance binding before pressing into a powder pellet. Pellets were analyzed on the Philips PW2400 X-ray fluorescence spectrometer equipped with a Rh X-ray tube. Calibration was based on 15 to 20 certified rock standards per element.

Phase-equilibrium modeling

Pseudosections were constructed in the nine-component chemical system $MnO–Na_2O–CaO–K_2O–FeO–MgO–Al_2O_3–SiO_2–H_2O$ (MnNaCaKFMASH) using the program THERMOCALC (v. 3.21), and the thermodynamic dataset of Holland & Powell (1998; data file created February 13, 2002). The nine-component chemical system was chosen because it can quantitatively predict the composition of garnet, biotite, and plagioclase during metamorphism (Vance & Mahar 1998, Tinkham *et al.* 2001). Equilibria were modeled with the mineral end-members and activity models presented in Tinkham *et al.* (2001), with the modifications presented in Stowell & Tinkham (2003).